


RESEARCH

Open Access

Hypoxia-challenged MSC-derived exosomes deliver miR-210 to attenuate post-infarction cardiac apoptosis



Hao Cheng^{1†} , Shufu Chang^{1†}, Rende Xu^{1†}, Lu Chen^{1†}, Xiaoyue Song¹, Jian Wu², Juying Qian¹, Yunzeng Zou² and Jianying Ma^{1*}

Abstract

Background: Myocardial infarction (MI) is a major cause of death worldwide. Although percutaneous coronary intervention and coronary artery bypass grafting can prolong life, cardiac damage persists. In particular, cardiomyocytes have no regenerative capacity. Mesenchymal stem cells (MSCs) are attractive candidates for the treatment of MI. The manner by which MSCs exert a beneficial effect upon injured cells is a source of continued study.

Methods: After the isolation and identification of exosomes from MSCs, the expression of miR-210 was determined by microarray chip. Subsequently, gain- and loss-function approaches were conducted to detect the role of exosomes and exosomal-miR-210 in cell proliferation and apoptosis of cardiomyocytes, as well as the MI in vivo. Dual-Luciferase Report Gene System was used to demonstrate the target gene of miR-210.

Results: We tested the hypothesis that MSC-derived exosomes transfer specific miRNA to protect cardiomyocytes from apoptotic cell death. Interestingly, direct cardiac injection of MSC exosomes reduced infarct size and improved heart function after coronary ligation. In vitro, the MSC exosomes enhanced cardiomyocyte survival to hypoxia. Confirmation of exosome uptake in myocytes was confirmed. Dual-luciferase reporter assay implicated miR-210 as a mediator of the therapeutic effect and AIFM3 as a downstream target. Treatment with miR-210 overexpressing MSC exosomes improved myocyte protection to both in vitro and in vivo stress. Furthermore, the endogenous and exogenous miR-210 had the same therapeutic effects.

Conclusion: These results demonstrated that the beneficial effects offered by MSC-exosomes transplantation after MI are at least partially because of excreted exosome containing mainly miR-210.

Keywords: Myocardial infarction, Exosome, Mesenchymal stem cells, Hypoxia, Apoptosis

* Correspondence: majianying@zs-hospital.sh.cn

[†]Hao Cheng, Shufu Chang, Rende Xu and Lu Chen contributed equally to this work.

¹Department of Cardiology, Zhongshan Hospital, Fudan University, 1609 Xietu Road, Shanghai 200032, China

Full list of author information is available at the end of the article



© The Author(s). 2020 **Open Access** This article is licensed under a Creative Commons Attribution 4.0 International License, which permits use, sharing, adaptation, distribution and reproduction in any medium or format, as long as you give appropriate credit to the original author(s) and the source, provide a link to the Creative Commons licence, and indicate if changes were made. The images or other third party material in this article are included in the article's Creative Commons licence, unless indicated otherwise in a credit line to the material. If material is not included in the article's Creative Commons licence and your intended use is not permitted by statutory regulation or exceeds the permitted use, you will need to obtain permission directly from the copyright holder. To view a copy of this licence, visit <http://creativecommons.org/licenses/by/4.0/>. The Creative Commons Public Domain Dedication waiver (<http://creativecommons.org/publicdomain/zero/1.0/>) applies to the data made available in this article, unless otherwise stated in a credit line to the data.

Background

Ischemic heart disease is a significant cause of morbidity and mortality [1]. Percutaneous coronary thrombolytic therapy improves clinical outcomes. However, nearly 25% of patients are not re-perfused in a timely manner [2]. Furthermore, cardiomyocytes have little to no regenerative capacity. Cell-based therapies, such as stem cells, which have regenerative potential, are being applied to individuals with cardiac disease [3]. Stem cells can secrete quantities of growth, anti-apoptotic, and anti-inflammatory factors that may improve heart function. However, technical issues have shown stem cells themselves to be inefficient [4]. Mesenchymal stem cells (MSCs) are prototypic adult stem cells [5] that produce paracrine growth factors that may increase survivability of cardiomyocytes and stimulate angiogenesis [6].

All cell types secrete membrane vesicles, including exosomes, that contain bioactive substances such as proteins, mRNAs, and miRNAs, and enzymes, among others [7]. During uptake by neighboring cells, exosome-delivered cargo has the potential to alter cell response [8]. Embryonic stem cell exosomes were reported to drive cardiac regeneration [9]. Others noted exosomes provided remote pre-conditioning to limit kidney injury [10]. Since prior studies have noted that MSC exosomes are cardio-protective, they are being tested as an off-the-shelf therapy for MI [11].

At the same time, MSC exosome treatment can alter miRNA levels [7]. miRNAs activated pro-survival kinases and induced a glycolytic switch to increase cellular resistance to hypoxic stress [12]. Post-MI individuals were found to have increased serum and decreased infarct tissue levels of miR-1 and miR-133a [13]. Parenthetically, miR-210 and miR-744 were found increased in exosomes in response to hypoxia. However, there was no miR-744 gene of rat in NCBI Gene. We chose miR-210 as our key role in myocardial protection. Furthermore, a number of studies have linked exosomal-miR-210 to protection from ischemic injury [14–16]. We hypothesized that MSCs secrete miRNA-210-enriched exosomes that, in a paracrine manner, protect cells and organs from injury. Herein, we show that exosome miR-210 limits hypoxia-driven myocyte apoptosis and tissue death following coronary ligation.

Methods

Animals

Animal experiments were approved by the Ethics Committee of Fudan University (reference number: 20140226-095). Wild type, male SD rats aged 10–12 weeks and newborn male SD rats were purchased from Shanghai Sippr-BK Laboratory Animal Co. Ltd. (Shanghai, China) and maintained under pathogen-free conditions.

Rat model of myocardium infarction and assessment of heart functions

Male SD rats (~250 g) were anesthetized with 10% chloral hydrate (w/v; Acros, Japan) by intraperitoneal injection. The heart was exposed and the left anterior descending artery ligated. Sham-ligated rats served as controls. Animals underwent injection of the cardiac muscle close to the area of arterial ligation with the following agents: PBS, exosomes derived from MSCs, exosomes derived from MSCs cultured in 10 μ M GW4869 that could inhibit exosome production sufficiently without toxic effects on cells [17], exosomes derived from MSCs infected with anti-miR-210, and exosomes from MSCs infected with empty lentivirus. The exosomes acquired from 1×10^6 MSCs were delivered in 20 μ l of PBS. Echocardiography was performed on days 0 and 28 after coronary ligation using a Vevo 2100 system (VisualSonics Inc., Toronto, ON, Canada) with an 80-MHz probe. Upon study completion, animals were euthanized, and tissues were harvested.

Cell isolation and culture

Bone mesenchymal stem cells were isolated from the femurs of SD rats and seeded onto culture dishes. Then they were cultured in DMEM/F12 supplemented with 10% fetal bovine serum (FBS; Invitrogen, Carlsbad, CA, USA) at 37 °C and 5% CO₂ until confluent. Medium was replaced every 2 days. At passage 3, the phenotype of MSCs was confirmed by flow cytometry using antibodies against rat CD90-APC and CD45-PEcy7 (#553080, BD Bioscience, San Diego, CA, USA). The SD Rat MSC Osteogenic Differentiation Basal Medium and Adipogenic Differentiation Basal Medium (Cyagen Bioscience, Guangzhou, China) were used to promote the differentiation of MSCs to further confirm differentiation capacity.

Exosome isolation

Exosomes from culture supernatants were isolated by ultracentrifugation. Collected cell culture supernatant was subjected to several centrifugations (300, 2000, and 10,000g for 15, 15, and 40 min, respectively). After each centrifugation, the supernatant was filtered through 0.22 μ m filters and the resultant was collected. Then the resultant was subjected to centrifugation at 110,000g for 75 min to yield a pellet that was suspended in PBS and then centrifuged again at 110,000g for 75 min. The pellet obtained with the final centrifugation was considered the exosomes.

A BCA assay kit (Beyotime, China) was used to analyze the protein level of lysed exosomes (50 μ l RIPA lysis buffer, Beyotime, China). CD63 and TSG101 protein levels were detected by Western blot. A mirVana miRNA isolation kit (Invitrogen, Austin, TX, USA) was

used to isolate exosome miRNA, and relative expression levels of miR-210 were determined by q-PCR.

Transmission electron microscopy

For electron microscopy analysis, exosome suspensions were absorbed onto formvar carbon-coated EM grids. Three grids were prepared for each exosome sample. An absorbing page was used to gently remove excess liquid. Then, the exosome suspension was subjected to 2.5% uranyl acetate staining for 7 min. Grids were washed three times with PBS and maintained in a semi-dry state. Samples were observed using a Hitachi-8100IV transmission electron microscope (Hitachi, Tokyo, Japan) at 100 kV.

Quantitative real-time PCR analysis

Total RNA was extracted from cells using TRIzol reagent (Invitrogen, Austin, TX, USA) following the manufacturer's instructions. Reverse-transcript reactions were conducted using the PrimeScript RT reagent kit (Takara, Japan). qPCR primers were purchased from Tiangen Biotech Co. Ltd. (Beijing, China). The has-miR-210 primers were CTGTGCGTGTGACAGCGGCTGA. qPCR was conducted using a standard SYBR Green PCR kit (Toyobo, Osaka, Japan) protocol on an Applied Biosystems 7500 Real-Time PCR System (Applied Biosystems, Foster City, CA, USA). The relative mRNA expression level was analyzed by the $2^{-\Delta\Delta CT}$ method.

Co-culture of cardiomyocytes and exosomes

Cardiomyocytes were isolated from newborn male SD rats with 1 mg/mL collagenase II (Invitrogen, Austin, TX, USA). After 3 days, the isolated cardiomyocytes were co-cultured with exosomes derived from MSCs, MSCs treated with GW4869, and MSCs transfected with miR-210 agomir, miR-210 antagomir, or negative vehicle. After 48 h, cardiomyocytes were collected for subsequent analyses.

Viability assay

Cell viability was evaluated by LDH-release assay (Beyotime, China) and CCK8 assay (Beyotime, China). Cardiomyocytes in 6-well plates were challenged with hypoxia \pm the indicated treatment. Culture supernatants were aliquoted to fresh 96-well plates with LDH-release assay buffer. Absorbance at 492 nm and 630 nm was measured with a Multi-Mode Microplate Reader (BioTek, Winooski, VT, USA) controlling for background signal. In other experiments, cells were treated as above and CCK8 reagent was added and absorbance at 450 nm measured.

Colocalization of miR210 and exosomes

Rat BMSCs P3 generation cells in good condition were digested with trypsin then centrifuged. The cells were

resuspended in complete medium and were spread in 4 wells of 6-well plate. The cell density will reach 80% next day. The cells were transfected with miR210 mimics. The transfection systems were (a) 125 μ l Opti-MEM + 7 μ l Lipofectamine3000; (b) 125 μ l Opti-MEM + 50 nM miR-210 mimics + 10 μ l P3000 Reagent. Twenty-four after transfection, the medium was replaced with low-glucose DMEM without FBS. The cells in 2 wells were placed in a 5% CO₂ incubator at 37 °C for 24 h; the cells in the other 2 wells were placed in an anoxic incubator for 24 h. The next day, the exosomes were isolated from the cell culture medium by ultracentrifugation. Then the exosomes were incubated with CD63 (1:100) and CD81 (1:100) at 4 °C overnight. After 24 h, the secondary antibodies were added and incubated in room temperature for 1 h in the dark. The secondary antibody corresponding to CD63 was goat anti-rabbit (1;100), blue fluorescence (Alexa Fluor 350); the secondary antibody corresponding to CD81 was donkey anti-mouse(1;100), red fluorescence (Alexa Fluor 555); and miR210 mimics come with green fluorescence (5'FAM). Finally, we used laser confocal microscope to observe and take pictures.

Exosomes endocytosis into cardiomyocytes

Rat Bone MSCs (BMSCs) P3 generation cells in good condition, were digested with trypsin then centrifuged. The cells were resuspended in complete medium and were spread in 2 wells of 6-well plate. The cell density will reach 80% the next day. The cells were transfected with miR210 mimics. The transfection systems and exosomes isolation procedures have been mentioned above. The exosomes were resuspended with high-glucose DMEM to make conditioned medium for cardiomyocytes. The cardiomyocytes were divided into 0 and 24 h culture groups. After reaching the time, the cell slides were removed and rinsed twice with PBS. It was treated with 4% paraformaldehyde under room temperature for 10 min and then rinsed with PBS three times, each 5 min. Then the 0.5% Txiton X-100 was added for 5 min under room temperature and rinsed with TBST three times, each 5 min. Next, the DAPI was treated for 10 min away from light and then rinsed with PBS three times, each 5 min. Finally, we used mount slides and took pictures under laser confocal microscope.

Dual-luciferase reporter assay

In order to construct the overexpression vector PGL3-AIFM3 promoter region, PCR primers were designed and synthesized based on the sequence information of the AIFM3 (NM_001013977.3) promoter region in the NCBI (see Supplemental Table 1). The AIFM3 promoter region was used for the PCR target gene, plus Kpn I/Xho I restriction sites at the 5' UTR of the AIFM3 promoter region-F and AIFM3 promoter region-R primers

to ligate to the vector PGL3. For analysis of luciferase activity, human embryonic kidney cells (HEK293T, ATCC) were cultured in 6-well plates and transfected. The transfection systems were (a) 150 μ l Opti-MEM + 4 μ l Lipofectamine2000 and (b) 150 μ l Opti-MEM + 3 μ l plasmid/50 nM miR-210/0.3 μ l RL-TK. The four groups were PGL3 + RL-TK, miR-210 + PGL3 + RL-TK, miR-210 + PGL3-AIFM3 + RL-TK, and miR-210 control + PGL3-AIFM3 + RL-TK. After growing 24 h, the cells were collected for application in the Dual-Luciferase Reporter Assay System (Beytime) using a GloMax 20/20 Luminometer (Promega, Winooski) under recommended condition. After lysed for 15 min at room temperature, renilla luciferase activity was employed as internal control, and the ratios of firefly luciferase luminescence relative to control were measured.

Western blot

All proteins from cells or myocardial tissue were extracted and quantified. Micro BCA™ Protein Assay Kits (Thermo Fisher Scientific, Waltham, MA) were used to quantify protein levels. Equivalent amounts of protein was electrophoresed through 12% SDS-PAGE (stacking gel, 70 V; separating gel, 110 V) and transferred to nitrocellulose membranes (200 mA, 50 min). Blots were incubated for 1 h at room temperature with the indicated antibodies (CD63: ab108950, 1:1000, Abcam, CA, USA; TSG101: ab125011, 1:5000, Abcam; Cleaved-Caspase-3: ab2302, 1:500, Abcam; Bcl-2: ab 196,495, 1:1000, Abcam; Bad: ab32445, 1:5000, Abcam; Bax: ab32503, 1:5000, Abcam), and then incubated

with goat-anti-rabbit/mouse HRP-linked secondary antibody (Abcam, Cambridge, MA, USA). Chemiluminescence substrate (Pierce Chemical, Rockford, IL, USA) was used to visualize protein signals. The intensity of the protein bands was analyzed by ImageJ software (NIH, USA).

Statistical analysis

All experiments were repeated at least three times. Data is shown as the mean \pm standard error. Statistical analysis was carried out using GraphPad Prism software (version 5.01; San Diego, CA, USA). The unpaired *t* test was used to compare data between groups. A *P* value < 0.05 was regarded as statistically significant.

Results

Preparation and characterization of hypoxia-challenged exosomes

Rat bone-derived MSCs were cultured for 72 h under hypoxia (1% O₂). Exosomes were isolated from MSC-conditioned medium and characterized by transmission electron micrography (TEM), Nanosight Tracking Analysis (NTA), and expression of the exosome surface markers (Fig. 1a–c). TEM showed that MSC-derived exosomes displayed a characteristic cup-shaped structure. NTA demonstrated exosome sizes ranged from 30 to 150 nm. Finally, Western blotting analysis of lysed exosomes detected the exosome markers, CD63 and TSG101. Furthermore, the secretion of exosome in the supernatant of MSCs cultured under hypoxia was

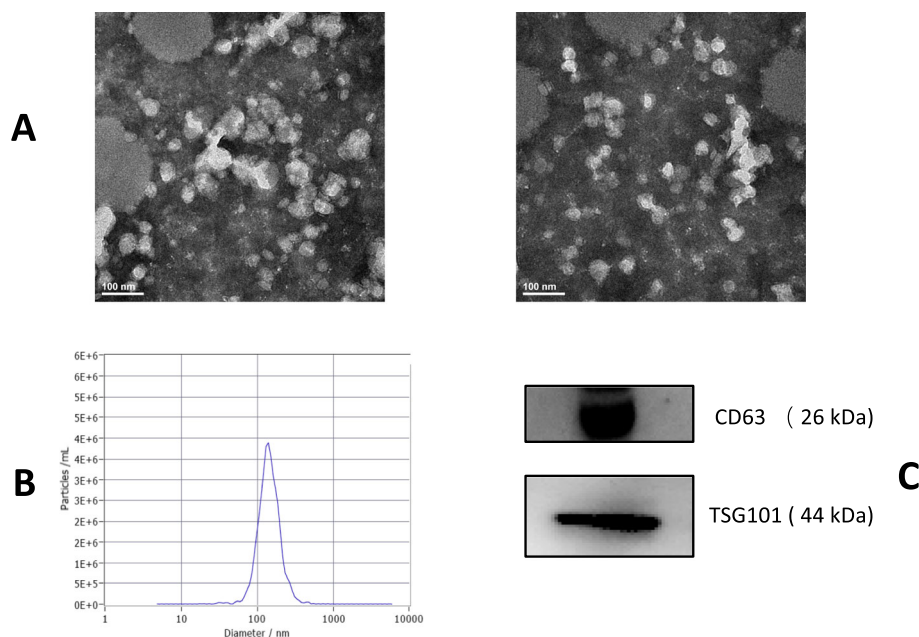


Fig. 1 Characterization of exosomes derived from MSCs. **a** Transmission electron micrographs of exosomes. Scale bar, 100 nm. Arrows, representative individual exosomes. **b** Nanoparticle Tracking Analysis (NTA) of exosomes. **c** Western blot analysis of CD63 and TSG101 expression in exosomes. Each experiment was repeated 3 times

significantly increased compared with that in normoxic culture (Supplemental Fig. 1A).

MSC exosomes protect against cardiomyocyte death

To test the potential of MSC exosomes to provide cardioprotection, we established a rodent model of MI. Upon coronary ligation, animals received the described treatments directly to the ischemic myocardium. Seven days post-injury, animals were euthanized and heart tissues were assessed for protein expression of several apoptosis-related genes (Cleaved-CASPASE-3, BAD, BAX, BCL-2). Cleaved-CASPASE-3 and BAX were increased in tissue samples from post-MI animals compared to sham-operated controls. Post-MI animals treated with MSC exosomes showed a decrease in levels of Cleaved-CASPASE-3, BAD, and BAX compared to controls. However, exosomes from MSCs cultured with GW4869, which limits exosome formation [17], did not decrease MI-related elevations in apoptosis proteins (Fig. 2a), suggesting a dose-dependent effect. Immunohistochemistry confirmed a significant decrease in the number of apoptotic cardiomyocytes in tissue samples from animals treated with exosomes versus those given MSCs-GW4869-exosomes or PBS (Fig. 2b).

MSC exosomes increase cardiomyocyte viability

Based on the above *in vivo* studies, we assessed the effects of MSC exosomes on cultured neonatal cardiomyocytes. MI is associated with profound cellular hypoxia. Therefore, we challenged cardiac neonatal myocytes with hypoxia and determined LDH levels as a maker of cell injury. Interestingly, hypoxic myocytes treated with exosomes released less LDH compared to hypoxia myocytes; this effect was lost in cells treated with exosomes from GW4869-exposed MSCs (Fig. 3a). Furthermore, MSC exosomes prevented the hypoxia-mediated decrease in myocyte viability. As expected, exosomes from GW4869-exposed MSCs did not limit the hypoxia-mediated decrease in myocyte viability (Fig. 3b). We hypothesized that hypoxia induced apoptosis in cultured myocytes. As seen in the micrographs, the number of TUNEL-positive myocytes was increased by hypoxia, which was abated when cells were co-treated with MSC exosomes (Fig. 3c). In this case, exosomes from GW4869-treated MSCs did not limit hypoxia-induced apoptosis (Fig. 3c). Similar to results in tissue samples from cardiac infarct regions, hypoxic cardiomyocytes showed increased protein expression of multiple apoptotic-associated genes as well as the programmed cell death mediator, caspase 3. These changes were abrogated when hypoxic myocytes were treated with MSC exosomes (Fig. 3d).

miR-210 is abundant in MSC exosomes and has protective effects

To identify the exosome cargoes possibly responsible for the therapeutic effects, we analyzed exosomal miRNAs.

Microarray screening found miR-201 to be differently increased in exosomes from hypoxic MSCs compared to normoxic MSC-derived exosomes (Supplemental Fig. 1B). Microarray results were confirmed by q-PCR (Fig. 4a). To determine if miR-201 was sufficient or necessary to the therapeutic exosome effect, we pretreated MSCs with a miR-210 oligonucleotide (MSC-exo^{miR-210}), anti-miR-210 oligonucleotide (MSC-exo^{anti-miR-210}), or a scrambled control (MSC-exo^{NC}) and harvested exosomes as described. Hypoxic myocytes treated with either regular MSC exosomes of MSC-exo^{miR-210} showed less LDH release and increased cell viability (on CCK8 assay) consistent with less injury (Fig. 4b). Conversely, cells treated with MSC-exo^{anti-miR-210} experienced increased cell injury and less viability (Fig. 4a, b). Similar results were observed on CCK-8 analysis and TUNEL assay among the cell treatment groups (Fig. 4c, d). Furthermore, BAX, BAD, and Cleaved-CASPASE 3 expression were higher in the hypoxia group compared to the MSC exosomes and MSC-exo^{miR-210} groups (Fig. 4e).

MSC-secreted exosomal-miR-210 provides increased cellular survival against the hypoxia-induced myocardium injury

To validate the protective effects of miR-210 *in vivo*, we induced cardiac ischemia via coronary ligation and injected at risk myocardium with either PBS, MSC-exo^{miR-210}, MSC-exo^{anti-miR-210}, or MSC-exo^{NC}. As detailed above, BAX, BAD, and Cleaved-CASPASE 3 levels were increased in tissue samples from the MI group. However, these effects were abolished when rats were treated with MSC-exo^{miR-210} (Fig. 5a). Conversely, treatment with MSC-exo^{anti-miR-210} did not alter injury-mediated increases in apoptotic-associated proteins (Fig. 5a). Apoptotic cells were increased in tissue samples from infarcted zones; this was less so in similar samples from animals treated with MSC-exo^{miR-210} (Fig. 5b).

Exosomal-miR-210 improves heart function and reduces cardiac fibrosis following coronary ligation

To further evaluate the protective effects of miR-210, we used echocardiography and PET-CT to assess the left ventricular ejection and changes in ventricular remodeling 4 weeks after myocardial infarction. Echocardiography revealed that the MSC-exo^{miR-210} treatment group, similar to the sham surgery animals, had improved cardiac performance and less dysfunctional ventricular remodeling compared to the MI-PBS group and the MSC-exo^{anti-miR-210} group (Fig. 6a–c). Figure 6a shows that post-injury MSC-exo^{miR-210}-treated rats had a significantly less decrease in ejection fraction (EF) ($44.36\% \pm 3.34\%$ vs. $25.21\% \pm 1.80\%$, $p < 0.05$) and less fractional shortening (FS) ($30.03\% \pm 1.68\%$ vs. $15.41\% \pm 1.53\%$, $p < 0.05$), with decreased left ventricular diastolic volume (LVIDd) (7.81 ± 0.50 mm vs.

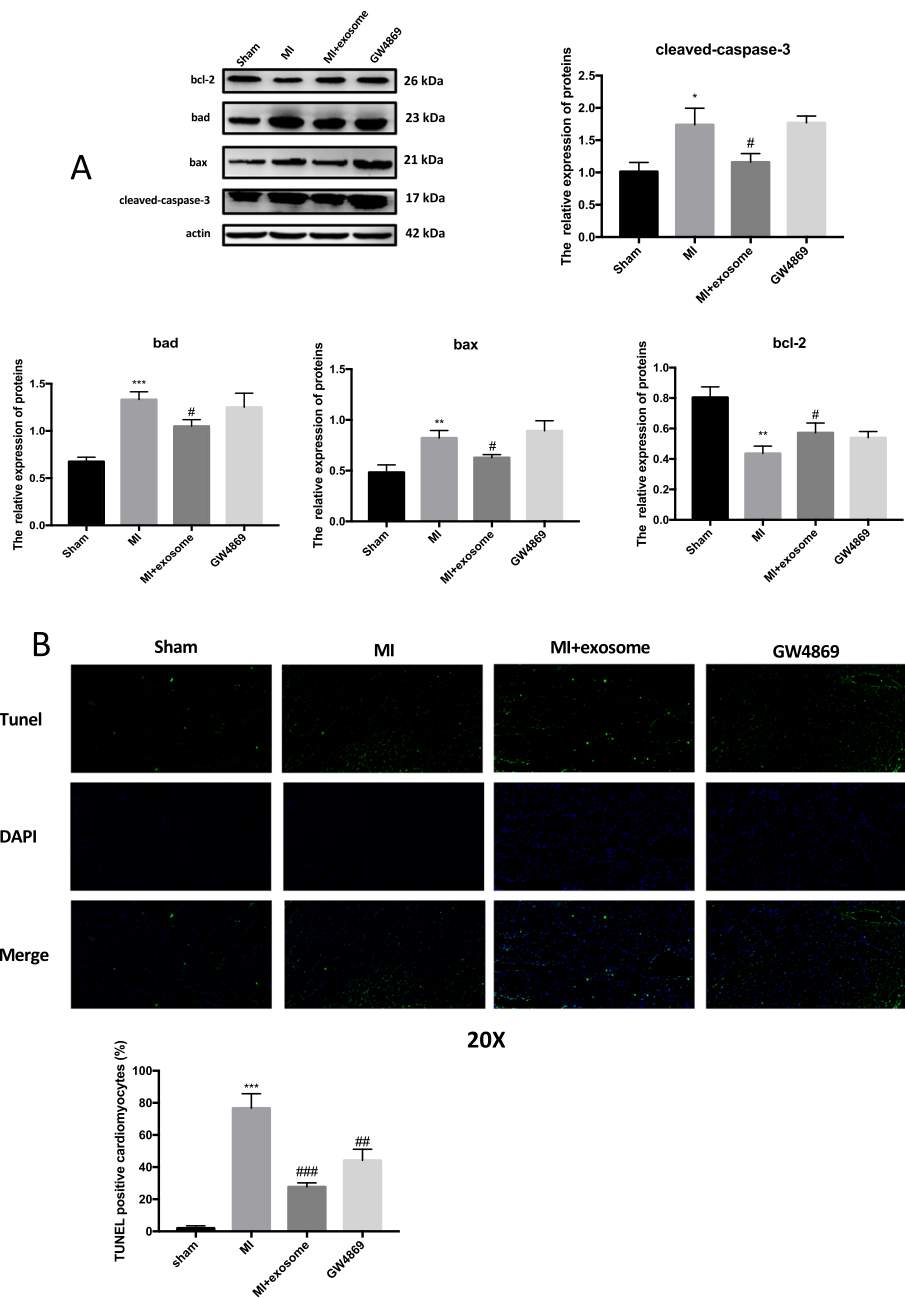


Fig. 2 Exosomes derived from MSCs inhibit apoptosis after myocardial infarction. **a** Expression levels of the apoptotic proteins BAD, BAX, BCL-2, and Cleaved-CASPASE-3 were evaluated in cardiac tissue sections from sham-operated rats and coronary-ligated rats that received either no therapy (PBS), MSC exosomes, or exosomes from MSCs treated after vessel occlusion with GW4869 immediately ($N = 5$ per group). Western blot analysis of protein lysates obtained from the infarct border zone. Quantitative analysis of BAD, BAX, BCL-2, and Cleaved-CASPASE-3 is shown in the lower panel. **b** Cell injury was determined by TUNEL assay. Fluorescence staining with vital dyes shown in blue indicates live cardiomyocytes, whereas ethidium homodimer-1 staining labels dead cells green. The percentage of cardiomyocytes death is shown in the right panels. Each experiment was repeated 3 times. * $p < 0.05$, ** $p < 0.01$, *** $p < 0.001$ for MI vs. sham. # $p < 0.05$ for MI + exosome vs. MI

11.05 ± 0.13 mm, $p < 0.001$) and LVIDs (6.66±0.32 mm vs. 8.89± 0.09 mm, $p < 0.001$), compared with MI-PBS-treated rats. PET-CT showed that the cardiac protective effects were much better in the MSC-exo^{miR-210} group than in the MSC-exo group (Fig. 5e). Lastly, infarct-

related tissue fibrosis (blue color on whole heart mounts) was significantly greater in the MSC-exo^{anti-miR-210} group than in rats treated with MSC-exo and MSC-exo^{miR-210} (Fig. 5d).

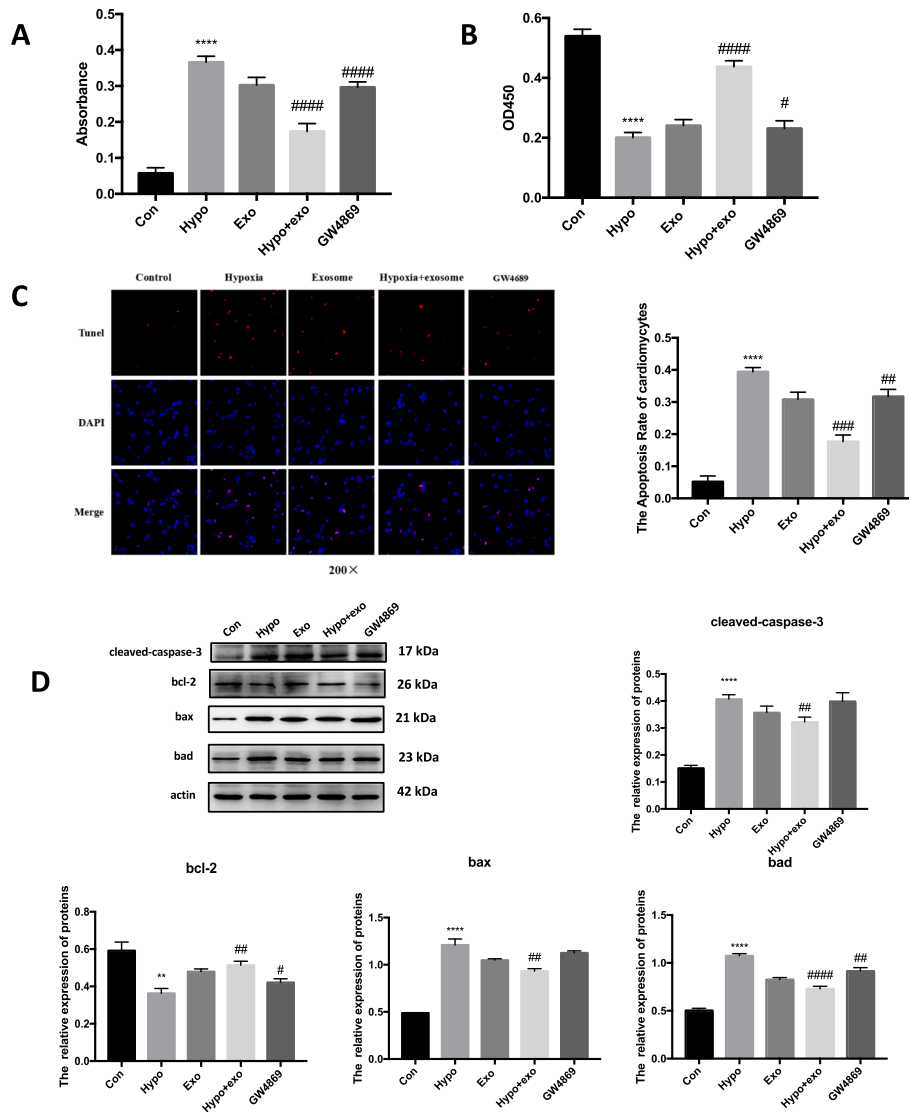


Fig. 3 Exosomes derived from MSCs reduce cell death. Hypoxic cardiomyocytes cultured in 1% O₂ for 24 h and treated with the indicate agents. Cells were divided into five groups: control group (cardiomyocytes were cultured in 21% O₂), hypoxia group (cardiomyocytes were cultured in 1% O₂), exosome group (exosomes were derived from MSC cultured in 21% O₂, and cardiomyocytes were cultured in 1% O₂), hypoxia + exosome group (exosomes were derived from MSC cultured in 1% O₂, and cardiomyocytes were cultured in 1% O₂), and GW4869 (MSCs were firstly treated with 10 μM GW4869, then exosomes were derived the MSCs and cardiomyocytes were cultured in 1% O₂). Cell injury was determined by LDH release assay (a), MTT assay (b) and TUNEL assay (c). Fluorescence staining with vital dyes shown in green indicates live cardiomyocytes, whereas ethidium homodimer-1 staining labels dead cells red. The percentage of cardiomyocytes death is shown in the right panels. d BAD, BAX, BCL-2, and Cleaved-CASPASE-3 levels were evaluated by Western blot and expression quantified. Each experiment was repeated 3 times. ***p* < 0.01, *****p* < 0.0001 for Hypo vs. Con. ####*p* < 0.0001 for hypo + exo or GW4869 vs. hypo

miR-210 regulates PI3K/AKT and p53 signaling by targeting AIFM3

While exosomes, and especially miR-201 over-expressing exosomes, improved cell and organ responses to stress, it was not clear if miR-201 was actually delivered to myocytes. Based on immunofluorescence microscopy, we detected co-localization of miR-210 within exosomes (Fig. 7a). Further confirmation of exosome endocytosis was obtained using continuous live cell

imaging of cardiomyocytes treated with conditioned medium enriched for MSC-exo^{miR-210} (Fig. 7b). miRNAs work at the post-transcriptional levels to regulate gene expression. According to the previous literatures and TargetScanHuman, an online prediction of microRNA targets (<http://www.targetscan.org/>), AIFM3 might be a target of miR-210 [18]. To test this hypothesis, dual-luciferase reporter assay was performed (Supplemental Fig. 2 and Table 1). Dual-luciferase reporter gene

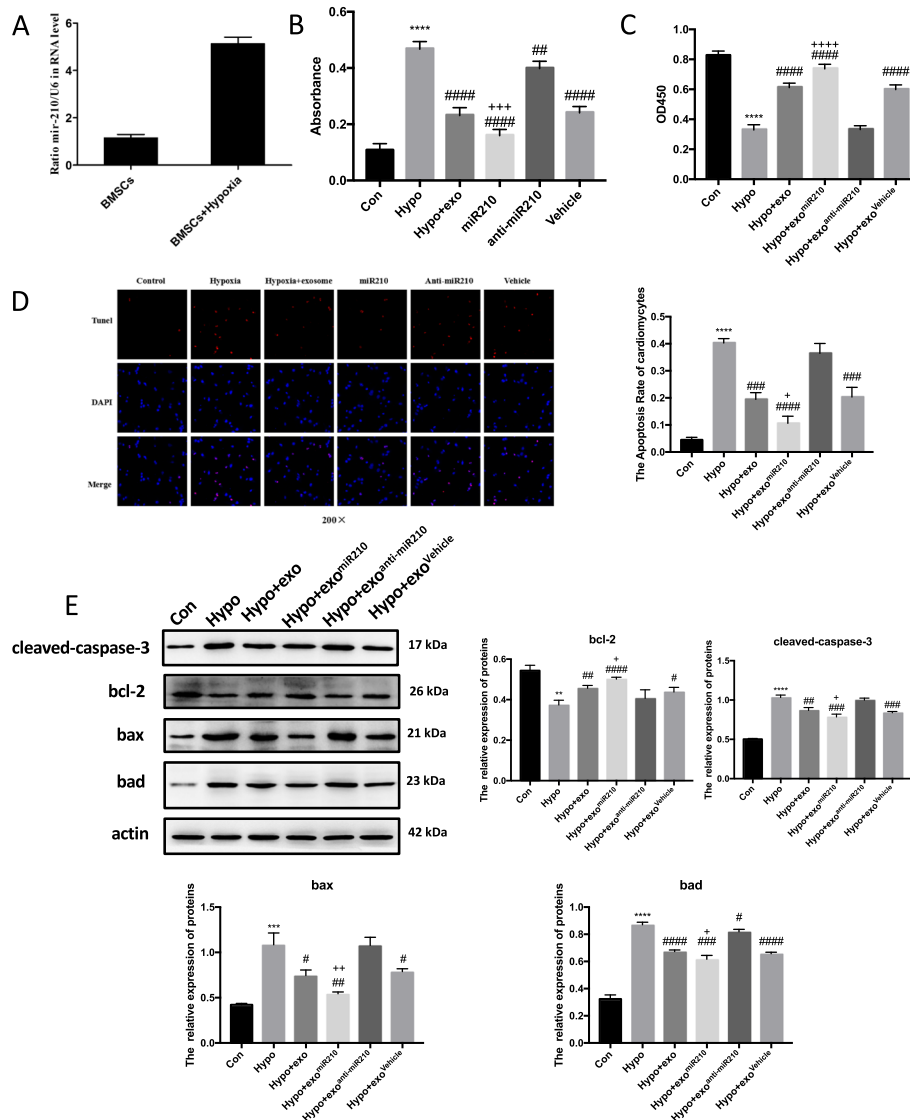


Fig. 4 Overexpression of miR210 in MSC exosomes strengthens their cardioprotective function in vitro. **a** Polymerase chain reaction quantification of miR210 in the exosomes obtained from MSCs. Hypoxic cardiomyocytes were treated with exosomes obtained from MSCs that were pre-treated with miR210 (exo^{miR210}), anti-miR210 (exo^{anti-miR210}), or scramble (exo^{Vehicle}) for the indicated time and cell injury characterized by LDH release (**b**), viability by MTT assay (**c**), and apoptotic programmed cell death by TUNEL assay (**d**). Red, TUNEL-positive nuclei; blue, DAPI-stained nuclei; green, troponin-positive cardiomyocytes. Scar bar $\times 200$. The percentage of TUNEL-positive cells is shown in the right panels. **e** Western blot identification of BAD, BAX, BCL-2, and Cleaved-CASPASE-3 in cardiomyocyte lysates after cell incubation with the indicated exosomes \pm hypoxia. Quantitative analysis of BAD, BAX, BCL-2, and Cleaved-CASPASE-3 is shown in the lower panel. Each experiment was repeated 3 times. $**p < 0.01$, $***p < 0.001$, $****p < 0.0001$ for hypo vs. con. $\#p < 0.05$, $\#\#p < 0.01$, $\#\#\#p < 0.001$, $\#\#\#\#p < 0.0001$ for hypo + exo, hypo + exo^{miR210}, hypo + exo^{anti-miR210} or hypo + exo^{Vehicle} vs. hypo. $+p < 0.05$, $++p < 0.01$, $+++p < 0.001$, $++++p < 0.0001$ for hypo + exo^{miR210} vs. hypo + exo

analysis of myocytes treated with MSC-exo^{miR-210} revealed that firefly luciferase activity was significantly inhibited when co-transfected with miR-210, indicating that AIFM3 as a down-stream target of miR-210 (Fig. 7c). We confirmed this result via Western blotting and q-PCR in miR-210 mimic-transfected cardiomyocytes. RNA levels of AIFM3 were significantly reduced in cardiomyocytes transfected with the miR-210 mimic

(Fig. 7d). Studies have linked AIFM3/p53 and PI3K/Akt signaling pathways in the setting of MI [18]. Therefore, we investigated the crosstalk between these two signaling pathways. Western blotting analysis suggested that levels AIFM3 were upregulated and levels of p-AKT, p-PI3K, and p-p53 were downregulated (Fig. 7c). After transfection with the miR-210 mimic, similar results were obtained (Fig. 7d).

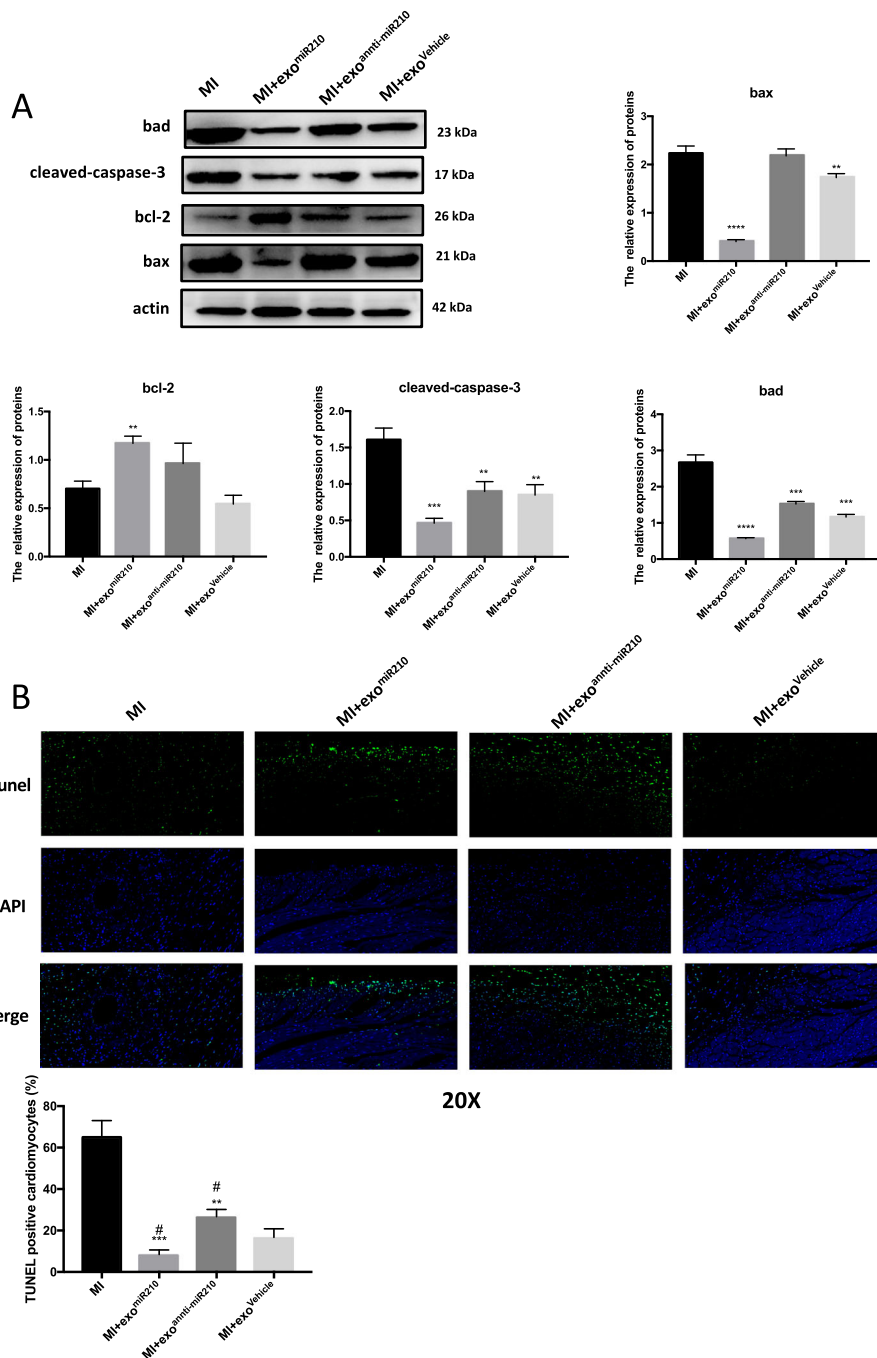
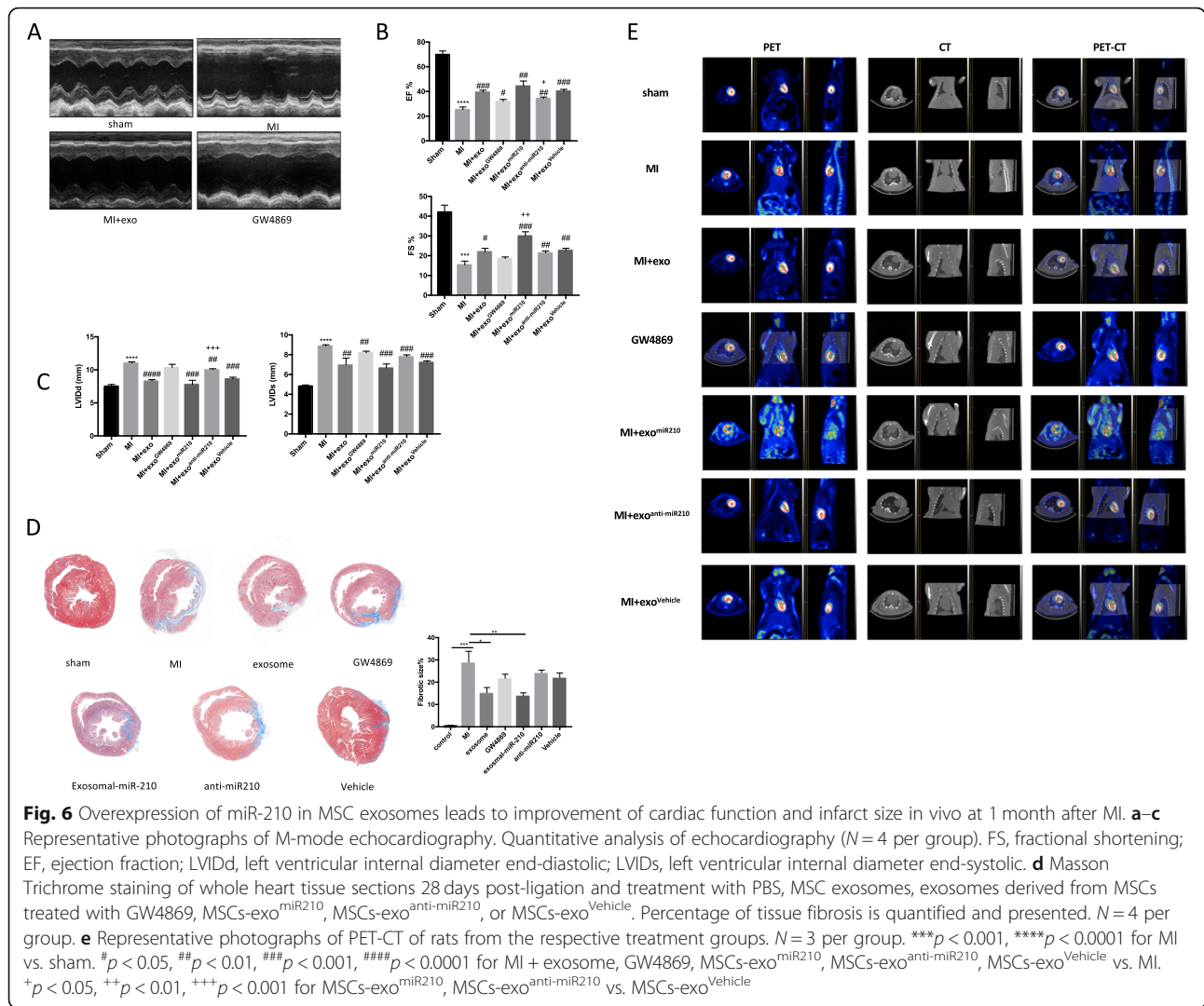


Fig. 5 Exosomes derived from MSCs with miR-210 overexpression inhibit apoptosis after myocardial infarction. **a** Western blot analysis of protein levels of apoptosis-associated genes BAD, BAX, BCL-2, and Cleaved-CASPASE-3 from cardiac tissue samples from mice in the indicated treatment groups. Each experiment was repeated 3 times. **b** Cell death in tissue samples was characterized by TUNEL assay. ** $p < 0.01$, *** $p < 0.001$, **** $p < 0.0001$ for MI + exo^{miR210}, MI + exo^{anti-miR210}, MI + exo^{Vehicle} vs. MI. # $p < 0.05$ for MI + exo^{miR210}, MI + exo^{anti-miR210} vs. MI + exo^{Vehicle}

The comparison of regulatory activity between endogenous and exogenous miR-210

To compare the regulatory activity between endogenous miR-210 and exogenous miR-210, we overexpressed the miR-210 in cardiomyocytes. Western blotting analysis revealed that expression levels of AIFM3, p-AKT, p-

PI3K, and p53 were downregulated in cardiomyocytes overexpressing miR-210 versus cardiomyocytes knocked-down for miR-210 (Fig. 8). Also, expression levels of BCL-2 were significantly upregulated, while the levels of Cleaved-CASPASE-3, BAD, and BAX were downregulated (Fig. 8).

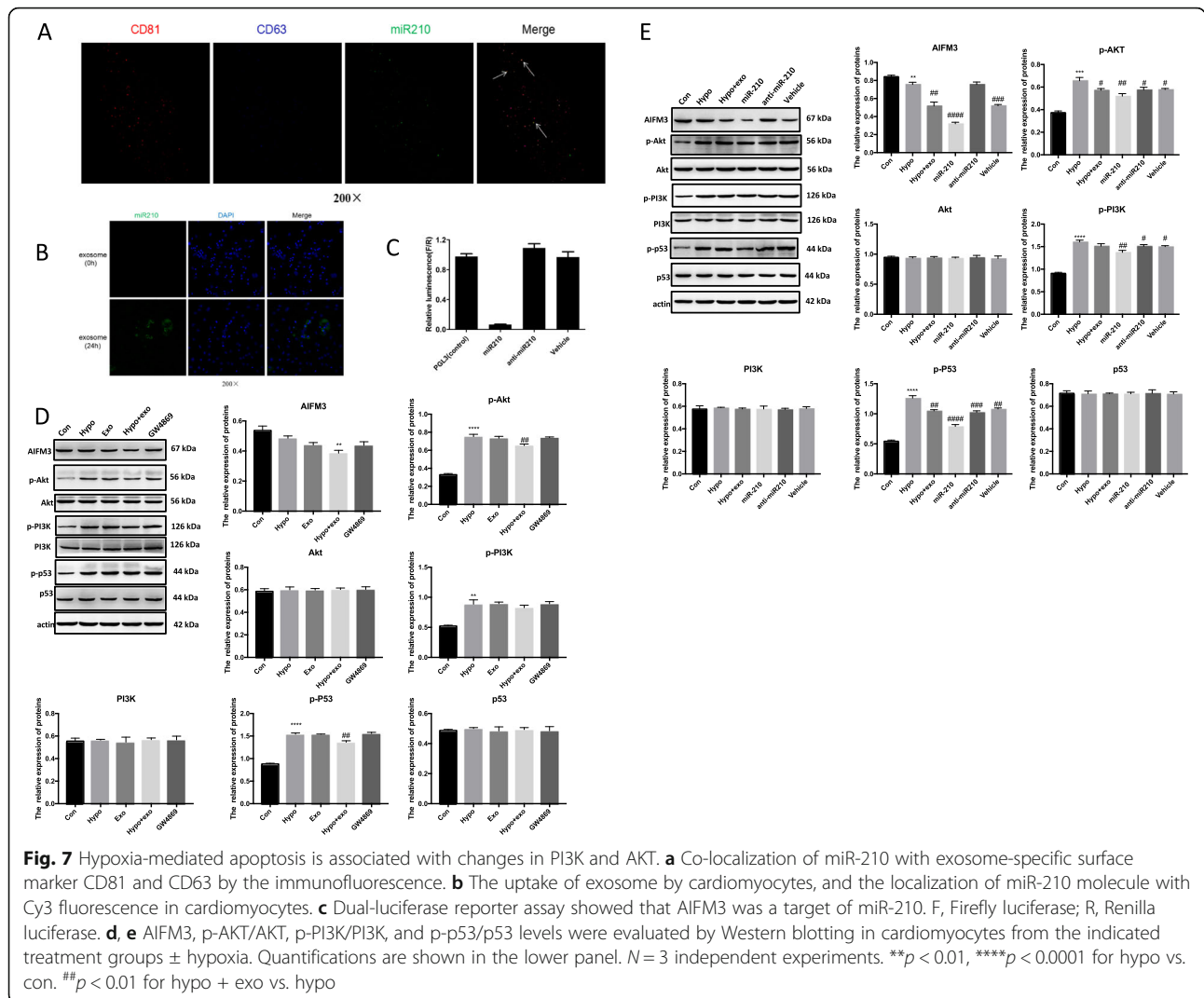


Discussion

Over the past decade, pioneering preclinical research into the use of cell therapy for cardiac regeneration has been completed [19]. However, cell therapy remains challenging for a number of reasons including the selection of cell types, the minimal potency of injected cells, and the limited engraftment and retention of administered cells [19–21]. A recent study demonstrated that although transplanted, cells could not differentiate into cardiac myocytes [22]. In this study, we have identified a mechanism by which the hypoxia-injured MSC “signals” to decrease apoptosis of ischemic cardiomyocytes. We have demonstrated that following MI, exosomes from MSC and their cargo miRNAs were protective for the cardiomyocytes. Notably, the transferred miR-210 down-regulates PI3K/Akt expression in the cardiomyocytes, resulting in apoptosis.

Not unexpectedly, exosomes, which have identified paracrine signaling capacities, are being considered as

possible therapies for a range of diseases. Consistent with our results, exosomes derived from MSCs prevented ventricular remodeling and reduced scarring in a mouse model of MI [11]. Extending these reports, we explored the possibility that exosome-mediated repair under these conditions relies on the transfer of miRNA. In support of this idea, others found that adipose tissue macrophages from obese mice secrete exosomal-miR-155 to promote glucose intolerance and insulin resistance [23]. miR-105 has been linked to sustained tumor growth [24]. Also, cancers can transfer activated epidermal growth receptor via exosomes to host macrophages and suppress innate antiviral immunity [25]. In this study, we used a miRNA array and found that MSC exosomes were enriched for miR-210. Of relevance to this finding, hypoxia has been reported to increase miR-210 [26]. In addition, it was reported that miR-210 promotes stabilization of carotid plaques via directly targeting the tumor suppressor gene adenomatous polyposis coli [16].



Similarly, increased expression of miR-210 enhanced the protective effects on Hypoxia/reoxygenation-injured endothelial cells [14]. Consistent with this, we observed that the treatment with MSC exosomal-miR-210 improved the survival of cardiomyocytes under the hypoxic condition in vitro and improved heart function in vivo and this was associated with changes in expression of the miR-210 target genes PI3K/Akt and p53. These results are in accordance with several studies suggesting that miR-210 has a protective function in cardiovascular disease through several mechanisms including SOCS1-STAT3-VEGF-C signaling [27]. Consistent with this finding, blocking the activity of nSMase2 lead to a reduction in miR-210 and abrogated any cardio-protective actions.

The regulation of AIFM3 by miR-210 has been reported in cardiomyocytes [28]. Likewise, we found that upregulation of exosomal-miR-210 decreased AIFM3, p-AKT, and p-p53. These effects were eliminated by the

knockdown of miR-210. Studies have found that miR-210 has other targets including PLK1, ISCU, Toll-like receptor, and Kruppel-like factor 7 [29–32]. Expanding on this data, we identified AIFM3 as a novel target of miR-210.

The relative contributions of endogenous and exogenous miRNAs in regulating cell responses are controversial. Most studies fail to demonstrate a function for endogenous exosomal miRNAs [33]. We directly overexpressed miR-210 in cardiomyocytes to compare the difference between the endogenous and induced miR-210 [34]. While our results suggest a possible role for endogenous exosomal miRNA, additional exploration of this is required.

This study has a number of limitations. First, the standardization of exosome harvest, handling, and characterization is ongoing [35]. As such, we selected one of several published approaches. While comparison of techniques would be ideal, this was not practical for

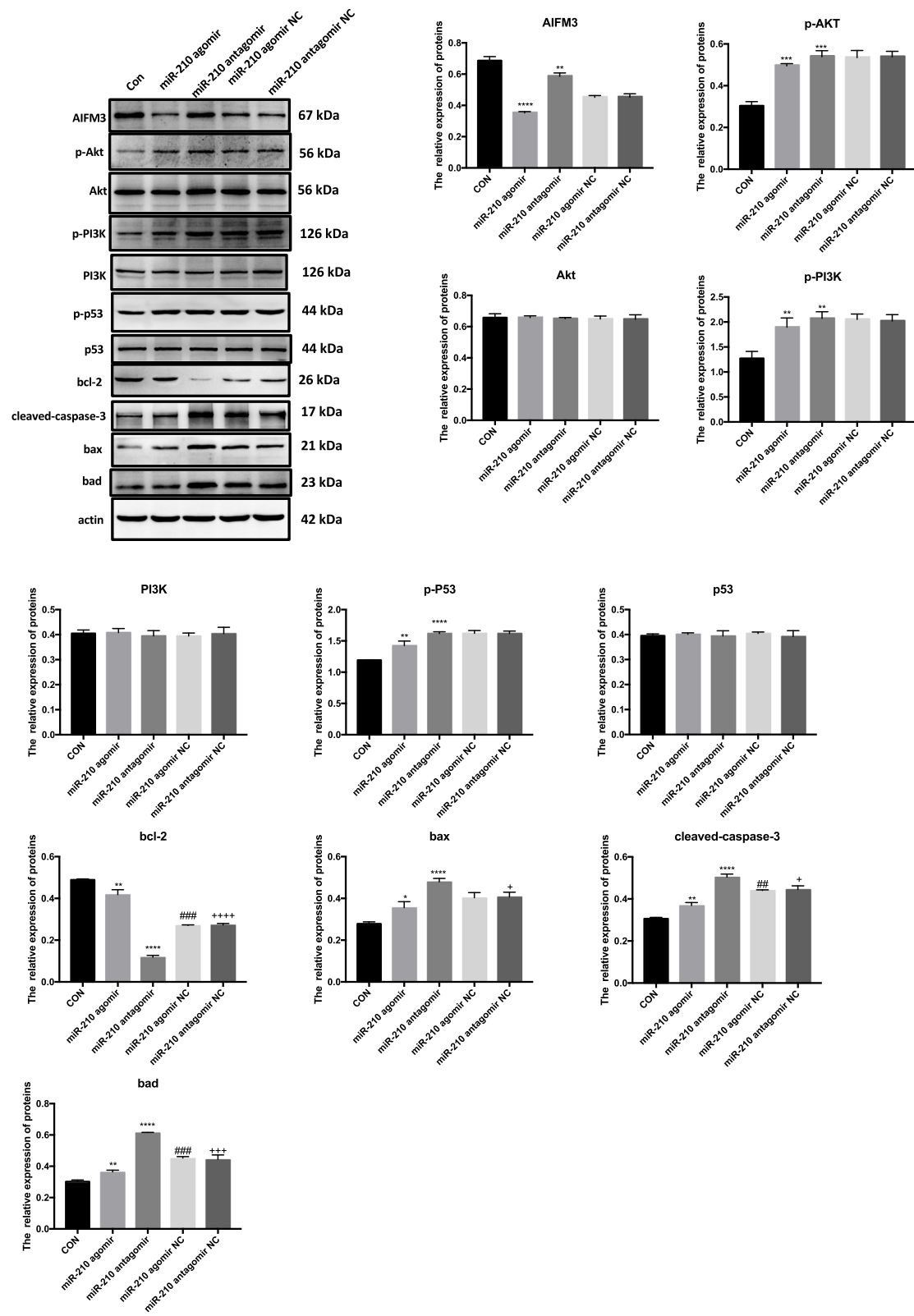


Fig. 8 (See legend on next page.)

(See figure on previous page.)

Fig. 8 Comparison of the uptake of exosomal miR-210 with the regulatory activity of endogenous miR-210. The protein levels of AIFM3, p-AKT/AKT, p-PI3K/PI3K, p-p53/p53, BAD, BAX, BCL-2, and Cleaved-CASPASE-3 were evaluated by Western blotting in cardiomyocytes treated with overexpressed miR-210. Quantifications are shown in the lower panel. $N = 3$ independent experiments. $**p < 0.01$, $***p < 0.001$, $****p < 0.0001$ for miR-210 agomir and miR-210 antagomir vs. con. $##p < 0.01$, $###p < 0.001$ for miR-210 agomir NC vs. miR-210 agomir. $+p < 0.05$, $+++p < 0.001$, $++++p < 0.0001$ for miR-210 antagomir NC vs. miR-210 antagomir

this study. Second, confocal imaging is not able to distinguish molecular proximity from interaction. Finally, exosomes express cell surface proteins, such as anti-angiogenic thrombospondin-1, that have profound signaling effects in the cardiovascular system. Thus, we cannot exclude the possible role of exosome membrane expressed molecules in our assays.

Conclusions

In conclusion, our study demonstrated the benefits associated with MSC exosomes after MI as well as a novel mechanism responsible for their anti-apoptotic effect via miR-210. Collectively, these results provide new insights into the mechanism of cell therapy and might be leveraged for the treatment of ischemic heart diseases.

Supplementary information

Supplementary information accompanies this paper at <https://doi.org/10.1186/s13287-020-01737-0>.

Additional file 1: Figure S1. Exosomes densities and miR-210 levels in different conditions.

Additional file 2: Figure S2. Successful construction of AIFM3 promoter report vector.

Additional file 3: Table S1. Primer used for PCR.

Abbreviations

MI: Myocardial infarction; MSC: Mesenchymal stem cell; BMSC: Bone mesenchymal stem cell; TEM: Transmission electron microscopy; NTA: Nanosight Tracking Analysis; FBS: Fetal bovine serum; PBS: Phosphate-buffered saline; RT-PCR: Reverse transcription-polymerase chain reaction; EF: L Ejection fraction; FS: Fractional shortening; LVIDd: Left ventricular end-diastolic internal diameters; LVIDs: Left ventricular end-systolic internal diameters

Acknowledgements

The authors acknowledge the Department of Cardiology, Zhongshan Hospital, Fudan University and Shanghai Institute of Cardiovascular Diseases. The manuscript has not been submitted elsewhere and is not under consideration for publication. All authors read and agreed with the submission of the manuscript. We give our sincere appreciation to the reviewers for their helpful comments on this article.

Authors' contributions

Hao Cheng, Shufu Chang, Rende Xu, and Lu Chen contributed equally to this work. Hao Cheng and Shufu Chang performed the experiments, analyzed the data, and wrote and revised manuscript. Rende Xu, Lu Chen, and Xiaoyue Song performed the experiments and analyzed the data. JianWu did the animal models and echocardiography and PET-CT. Yunzeng Zou and Juying Qian provided some suggestions. Jianying Ma designed the experiments and wrote and revised manuscript. The authors read and approved the final manuscript.

Funding

This work was supported by the grants from National Basic Research Program of China (No. 81470467).

Availability of data and materials

All data generated or analyzed in this study are included in this article (and its supplementary information files).

Ethics approval and consent to participate

This study was conducted under the approval of the Department of Cardiology, Zhongshan Hospital, Fudan University and Shanghai Institute of Cardiovascular Diseases. Animal experiments were conducted under the approval of the Animal Ethics Committee of Zhongshan Hospital, Fudan University. Treatment of experimental animals followed the internationally recognized 3R principle, which is the replacement, reduction, and refinement of experimental animals. Moreover, the protocols involved experimental animals followed the welfare ethics of the experimental animals according to the requirements of the guidelines for ethical review of experimental animal welfare (GB/T 35892-2018) of China.

Consent for publication

Not applicable.

Competing interests

The authors declare that they have no competing interests.

Author details

¹Department of Cardiology, Zhongshan Hospital, Fudan University, 1609 Xietu Road, Shanghai 200032, China. ²Shanghai Institute of Cardiovascular Diseases, Zhongshan Hospital and Institute of Biomedical Sciences, Fudan University, 180 Feng Lin Road, Shanghai 20032, China.

Received: 18 March 2020 Revised: 14 April 2020

Accepted: 19 May 2020 Published online: 08 June 2020

References

- Benjamin EJ, Muntner P, Alonso A, Bittencourt MS, Callaway CW, Carson AP, Chamberlain AM, Chang AR, Cheng S, Das SR, Delling FN, Djousse L, Elkind MSV, Ferguson JF, Fornage M, Jordan LC, Khan SS, Kissela BM, Knutson KL, Kwan TW, Lackland DT, Lewis TT, Lichtman JH, Longenecker CT, Loop MS, Lutsey PL, Martin SS, Matsushita K, Moran AE, Mussolino ME, O'Flaherty M, Pandey A, Perak AM, Rosamond WD, Roth GA, Sampson UKA, Satou GM, Schroeder EB, Shah SH, Spartano NL, Stokes A, Tirschwell DL, Tsao CW, Turakhia MP, VanWagner LB, Wilkins JT, Wong SS, Virani SS, Epid AHAC, Comm PS, Subcomm SS. Heart Disease and Stroke Statistics-2019 Update A Report From the American Heart Association. *Circulation*. 2019;139:E56–E528.
- Cohen M, Boiangiu C, Abidi M. Therapy for ST-segment elevation myocardial infarction patients who present late or are ineligible for reperfusion therapy. *J Am Coll Cardiol*. 2010;55:1895–906.
- Dias LD, Casali KR, Ghem C, da Silva MK, Sausen G, Palma PB, Covas DT, Kalil RAK, Schaan BD, Nardi NB, Markoski MM. Mesenchymal stem cells from sternum: the type of heart disease, ischemic or valvular, does not influence the cell culture establishment and growth kinetics. *J Transl Med*. 2017;15:161.
- Vrijns KR, Maring JA, Chamuleau SA, Verhage V, Mol EA, Deddens JC, Metz CH, Lodder K, van Eeuwijk EC, van Dommelen SM, Doevendans PA, Smits AM, Goumans MJ, Sluijter JP. Exosomes from cardiomyocyte progenitor cells and mesenchymal stem cells stimulate angiogenesis via ENMPRIN. *Adv Healthc Mater*. 2016;5:2555–65.
- Williams AR, Hare JM. Mesenchymal stem cells biology, pathophysiology, translational findings, and therapeutic implications for cardiac disease. *Circ Res*. 2011;109:923–40.

6. Shafei AE, Ali MA, Ghanem HG, Shehata AI, Abdelgawad AA, Handal HR, Talaat KA, Ashaal AE, El-Shal AS. Mesenchymal stem cell therapy: a promising cell-based therapy for treatment of myocardial infarction. *J Gene Med.* 2017;19:e2995.
7. Zhang ZW, Yang JJ, Yan WY, Li YX, Shen ZY, Asahara T. Pretreatment of cardiac stem cells with exosomes derived from mesenchymal stem cells enhances myocardial repair. *J Am Heart Assoc.* 2016;5:e002856.
8. Suzuki E, Fujita D, Takahashi M, Oba S, Nishimatsu H. Stem cell-derived exosomes as a therapeutic tool for cardiovascular disease. *World J Stem Cells.* 2016;8:297–305.
9. Khan M, Nickloff E, Abramova T, Johnson J, Verma SK, Krishnamurthy P, Mackie AR, Vaughan E, Garikipati VN, Benedict C, Ramirez V, Lambers E, Ito A, Gao E, Misener S, Luongo T, Elrod J, Qin G, Houser SR, Koch WJ, Kishore R. Embryonic stem cell-derived exosomes promote endogenous repair mechanisms and enhance cardiac function following myocardial infarction. *Circ Res.* 2015;117:52–64.
10. Pan T, Jia P, Chen N, Fang Y, Liang Y, Guo M, Ding X. Delayed remote ischemic preconditioning Confers Renoprotection against septic acute kidney injury via exosomal miR-21. *Theranostics.* 2019;9:405–23.
11. Arslan F, Lai RC, Smeets MB, Akeroyd L, Choo A, Aguor ENE, Timmers L, van Rijen HV, Doevendans PA, Pasterkamp G, Lim SK, de Kleijn DP. Mesenchymal stem cell-derived exosomes increase ATP levels, decrease oxidative stress and activate PI3K/Akt pathway to enhance myocardial viability and prevent adverse remodeling after myocardial ischemia/reperfusion injury. *Stem Cell Res.* 2013;10:301–12.
12. Ong SG, Lee WH, Huang M, Dey D, Kodo K, Sanchez-Freire V, Gold JD, Wu JC. Cross talk of combined gene and cell therapy in ischemic heart disease role of exosomal microRNA transfer. *Circulation.* 2014;130:560.
13. Kuwabara Y, Ono K, Horie T, Nishi H, Nagao K, Kinoshita M, Watanabe S, Baba O, Kojima Y, Shizuta S, Imai M, Tamura T, Kita T, Kimura T. Increased microRNA-1 and microRNA-133a levels in serum of patients with cardiovascular disease indicate myocardial damage. *Circ-Cardiovasc Gene.* 2011;4:446–U287.
14. Ma XT, Wang JJ, Li J, Ma CL, Chen SZ, Lei W, Yang Y, Liu SM, Bihl J, Chen C. Loading MiR-210 in endothelial progenitor cells derived exosomes boosts their beneficial effects on hypoxia/eoxygenation-injured human endothelial cells via protecting mitochondrial function. *Cell Physiol Biochem.* 2018;46:664–75.
15. Zaccagnini G, Maimone B, Fuschi P, Maselli D, Spinetti G, Gaetano C, Martelli F. Overexpression of miR-210 and its significance in ischemic tissue damage. *Sci Rep-Uk.* 2017;7:9563.
16. Eken SM, Jin H, Chernogubova E, Li YH, Simon N, Sun CY, Korzunowicz G, Busch A, Backlund A, Osterholm C, Razuvaev A, Renne T, Eckstein HH, Pelisek J, Eriksson P, Diez MG, Matic LP, Schellinger IN, Raaz U, Leeper NJ, Hansson GK, Paulsson-Berne G, Hedin U, Maegdefessel L. MicroRNA-210 enhances fibrous cap stability in advanced atherosclerotic lesions. *Circ Res.* 2017;120:633.
17. Essandoh K, Yang L, Wang X, Huang W, Qin D, Hao J, Wang Y, Zingarelli B, Peng T, Fan GC. Blockade of exosome generation with GW4869 dampens the sepsis-induced inflammation and cardiac dysfunction. *Biochim Biophys Acta.* 2015;1852:2362–71.
18. Mutharasan RK, Nagpal V, Ichikawa Y, Ardehali H. microRNA-210 is upregulated in hypoxic cardiomyocytes through Akt- and p53-dependent pathways and exerts cytoprotective effects. *Am J Physiol Heart Circ Physiol.* 2011;301:H1519–30.
19. Braunwald E. Cell-based therapy in cardiac regeneration: an overview. *Circ Res.* 2018;123:132–7.
20. Broughton KM, Sussman MA. Enhancement strategies for cardiac regenerative cell therapy: focus on adult stem cells. *Circ Res.* 2018;123:177–87.
21. Banerjee MN, Bolli R, Hare JM. Clinical studies of cell therapy in cardiovascular medicine: recent developments and future directions. *Circ Res.* 2018;123:266–87.
22. Tang XL, Li QH, Rokosh G, Sanganalmath SK, Chen N, Ou QH, Stowers H, Hunt G, Bolli R. Long-term outcome of administration of c-kit(POS) cardiac progenitor cells after acute myocardial infarction transplanted cells do not become cardiomyocytes, but structural and functional improvement and proliferation of endogenous cells persist for at least one year. *Circ Res.* 2016;118:1091–105.
23. Ying W, Riopel M, Bandyopadhyay G, Dong Y, Birmingham A, Seo JB, Ofrecio JM, Wollam J, Hernandez-Carretero A, Fu WX, Li PP, Olefsky JM. Adipose tissue macrophage-derived exosomal miRNAs can modulate in vivo and in vitro insulin sensitivity. *Cell.* 2017;171:372.
24. Yan W, Wu X, Zhou W, Fong MY, Cao M, Liu J, Liu X, Chen CH, Fadare O, Pizzo DP, Wu J, Liu L, Liu X, Chin AR, Ren X, Chen Y, Locasale JW, Wang SE. Cancer-cell-secreted exosomal miR-105 promotes tumour growth through the MYC-dependent metabolic reprogramming of stromal cells. *Nat Cell Biol.* 2018;20:597–609.
25. Gao L, Wang L, Dai T, Jin K, Zhang Z, Wang S, Xie F, Fang P, Yang B, Huang H, van Dam H, Zhou F, Zhang L. Tumor-derived exosomes antagonize innate antiviral immunity. *Nat Immunol.* 2018;19:233–45.
26. Wang H, Flach H, Onizawa M, Wei L, McManus MT, Weiss A. Negative regulation of Hif1a expression and TH17 differentiation by the hypoxia-regulated microRNA miR-210. *Nat Immunol.* 2014;15:393–401.
27. Meng ZY, Kang HL, Duan W, Zheng J, Li QN, Zhou ZJ. MicroRNA-210 promotes accumulation of neural precursor cells around ischemic foci after cerebral ischemia by regulating the SOCS1-STAT3-VEGF-C pathway. *J Am Heart Assoc.* 2018;7:e005052.
28. Ke X, Yan R, Sun Z, Cheng Y, Meltzer A, Lu N, Shu X, Wang Z, Huang B, Liu X, Wang Z, Song JH, Ng CK, Ibrahim S, Abraham JM, Shin EJ, He S, Meltzer SJ. Esophageal adenocarcinoma-derived extracellular vesicle microRNAs induce a neoplastic phenotype in gastric organoids. *Neoplasia.* 2017;19:941–9.
29. Li C, Zhou X, Wang Y, Jing S, Yang C, Sun G, Liu Q, Cheng Y, Wang L. miR210 regulates esophageal cancer cell proliferation by inducing G2/M phase cell cycle arrest through targeting PLK1. *Mol Med Rep.* 2014;10:2099–104.
30. Lu Y, Huang J, Geng S, Chen H, Song C, Zhu S, Zhao S, Yuan M, Li X, Hu H. MitoKATP regulating HIF/miR210/ISCU signaling axis and formation of a positive feedback loop in chronic hypoxia-induced PAH rat model. *Exp Ther Med.* 2017;13:1697–701.
31. Li C, Zhao M, Zhang C, Zhang W, Zhao X, Duan X, Xu W. miR210 modulates respiratory burst in *Apostichopus japonicus* coelomocytes via targeting toll-like receptor. *Dev Comp Immunol.* 2016;65:377–81.
32. Lv JX, Zhou J, Tong RQ, Wang B, Chen XL, Zhuang YY, Xia F, Wei XD. Hypoxia-induced miR210 contributes to apoptosis of mouse spermatocyte GC2 cells by targeting Kruppel-like factor 7. *Mol Med Rep.* 2019;19:271–9.
33. Xiao C, Wang K, Xu Y, Hu H, Zhang N, Wang Y, Zhong Z, Zhao J, Li Q, Zhu D, Ke C, Zhong S, Wu X, Yu H, Zhu W, Chen J, Zhang J, Wang J, Hu X. Transplanted mesenchymal stem cells reduce autophagic flux in infarcted hearts via the exosomal transfer of miR-125b. *Circ Res.* 2018;123:564–78.
34. Paul P, Chakraborty A, Sarkar D, Langthasa M, Rahman M, Singha RKS, Malakar AK, Chakraborty S. Interplay between miRNAs and human diseases. *J Cell Physiol.* 2018;233:2007–18.
35. Witwer KW, Van Balkom BWM, Bruno S, Choo A, Dominici M, Gimona M, Hill AF, De Kleijn D, Koh M, Lai RC, Mitsialis SA, Ortiz LA, Rohde E, Asada T, Toh WS, Weiss DJ, Zheng L, Giebel B, Lim SK. Defining mesenchymal stromal cell (MSC)-derived small extracellular vesicles for therapeutic applications. *J Extracell Vesicles.* 2019;8:1609206.

Publisher's Note

Springer Nature remains neutral with regard to jurisdictional claims in published maps and institutional affiliations.

Ready to submit your research? Choose BMC and benefit from:

- fast, convenient online submission
- thorough peer review by experienced researchers in your field
- rapid publication on acceptance
- support for research data, including large and complex data types
- gold Open Access which fosters wider collaboration and increased citations
- maximum visibility for your research: over 100M website views per year

At BMC, research is always in progress.

Learn more biomedcentral.com/submissions

